

Characterization of $\text{NdSrCo}_{1-x}\text{Fe}_x\text{O}_{4+\delta}$ ($0 \leq x \leq 1.0$) intergrowth oxide cathode materials for intermediate temperature solid oxide fuel cells

Ki-Woog Song^a, Ki-Tae Lee^{a,b,*}

^a Division of Advanced Materials Engineering, Chonbuk National University, Jeonbuk 560-756, Republic of Korea

^b Hydrogen and Fuel Cell Research Center, Chonbuk National University, Jeonbuk 560-756, Republic of Korea

Received 2 August 2010; received in revised form 12 August 2010; accepted 25 September 2010

Available online 28 October 2010

Abstract

$\text{NdSrCo}_{1-x}\text{Fe}_x\text{O}_{4+\delta}$ ($0 \leq x \leq 1.0$) intergrowth oxides have been investigated as cathode materials for intermediate temperature solid oxide fuel cells (IT-SOFCs). All the cathodes prepared by a glycine nitrate process (GNP) indicated single phase intergrowth oxides. The introduction of Fe for Co leads to decrease TEC values and electrical conductivity, and increase polarization resistance and oxygen content. The polarization resistance of $\text{NdSrCoO}_{4+\delta}$ composition is $0.16 \, \Omega \, \text{cm}^2$ at $800 \, ^\circ\text{C}$ in air atmosphere, which is the best electrochemical performance compared with other compositions.

© 2010 Elsevier Ltd and Techna Group S.r.l. All rights reserved.

Key words: C. Thermal expansion; Solid oxide fuel cell; Cathode; Oxygen reduction reaction

1. Introduction

IT-SOFCs suffer with low electrochemical performance which is mainly attributed to a cathode due to poor catalytic activity for the oxygen reduction reaction at low temperature [1,2]. Therefore it is important for cathode materials to improve the kinetics of oxygen reduction. In this regard, the cathode materials need to possess both electronic and ionic conductivities to show adequate catalytic activity for oxygen reduction [1,2].

Recently, perovskite related intergrowth oxides that belong to the Ruddlesden–Popper (R–P) series with the general formula $A_{n+1}B_nO_{3n+1}$ have been studied for IT-SOFCs, since the R–P series exhibit high oxide ion and electronic conductivities [3,4–6]. Among the R–P series, some interest has been focused on the $n = 1$ intergrowth oxides with good catalytic activity for oxygen and relatively low thermal expansion coefficient (TEC) compared to other cathode materials [6–10]. In this study, $\text{NdSrCo}_{1-x}\text{Fe}_x\text{O}_{4+\delta}$ intergrowth oxides as $n = 1$ R–P series have been investigated for IT-SOFCs.

2. Experimental

$\text{NdSrCo}_{1-x}\text{Fe}_x\text{O}_{4+\delta}$ intergrowth oxides were synthesized by glycine nitrate process (GNP). The required amount of metal nitrates and glycine was dissolved in distilled water. After sufficient stirring, the mixed solution containing glycine and nitrates were heated and concentrated until it turned to a viscous liquid under $100 \, ^\circ\text{C}$. The viscous liquid was heated to around $250 \, ^\circ\text{C}$ until a spontaneous combustion of the liquid occurred, afterward it formed foamy and fragile mass. After completing the GNP, the ignited mass was calcined at $1200 \, ^\circ\text{C}$ for 12 h.

The phase identification of the prepared powders was carried out by analyzing the X-ray diffraction data. Iodometric titration was conducted to determine the concentration of oxide ion vacancies and average oxidation state of the transition metal ions at room temperature. The thermal expansion coefficients (TECs) of the sintered samples were measured by a thermomechanical analysis (TMA) from room temperature to $700 \, ^\circ\text{C}$ with a heating rate of $10 \, ^\circ\text{C}/\text{min}$. The electrical conductivity was measured by a four-probe dc method in the temperature range of 100 – $800 \, ^\circ\text{C}$. For the electrical conductivity and TEC measurements, the samples were sintered at $1300 \, ^\circ\text{C}$ for 12 h, while the $x = 0$ composition was not sintered as a crack free sample. All the samples used for conductivity

* Corresponding author. Tel.: +82 63 270 2290; fax: +82 63 270 2386.

E-mail address: ktlee71@jbnu.ac.kr (K.-T. Lee).

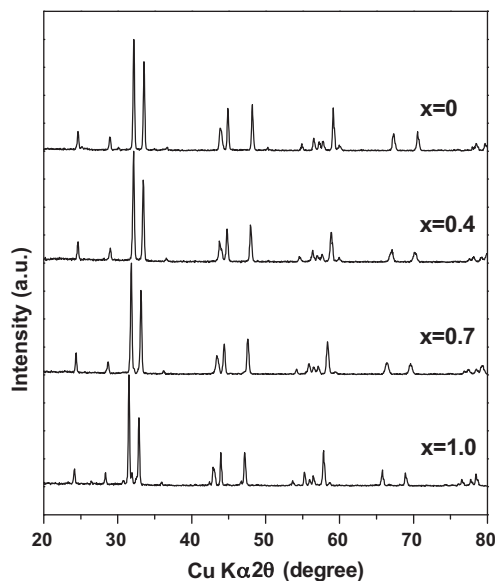


Fig. 1. X-ray diffraction patterns of the $\text{NdSrCo}_{1-x}\text{Fe}_x\text{O}_{4+\delta}$ cathodes calcined at 1200°C for 12 h.

and TEC measurements had densities of $>95\%$ of the theoretical values.

The electrochemical performance was evaluated by AC impedance spectroscopy with symmetrical half cells in various atmospheres. The applied frequency was in the range of 1 mHz to 100 kHz with the voltage amplitude of 20 mV. Symmetric half cells were manufactured by screen printing method, followed by firing at 1000°C for 2 h.

3. Results and discussion

The X-ray diffraction patterns of the $\text{NdSrCo}_{1-x}\text{Fe}_x\text{O}_{4+\delta}$ oxide cathodes prepared by glycine nitrate process (GNP) and fired at 1200°C for 12 h, are shown in Fig. 1. All patterns indicate K_2NiF_4 type structure as a perovskite related intergrowth oxide.

The average oxidation state values of the transition metal ions on B site of intergrowth oxide structure and the oxygen contents determined by the iodometric titration at room temperature are listed in Table 1. Nd and Sr ions are fixed valence state of $3+$ and $2+$ in the structure, respectively, thus Co and Fe ions need to exist as $3+$ valence state to make charge compensation. The results in Table 1 refer that all cathode materials possess excess oxide ions, and Co^{4+} ions somewhat

Table 1
Oxygen content ($4+\delta$) and B site mean valence data measured by iodometric titration at room temperature.

Composition	Mean valence of B site cations	Oxygen content ($4+\delta$)
$\text{NdSrCoO}_{4+\delta}$	3.04	4.02
$\text{NdSrCo}_{0.6}\text{Fe}_{0.4}\text{O}_{4+\delta}$	3.10	4.05
$\text{NdSrCo}_{0.3}\text{Fe}_{0.7}\text{O}_{4+\delta}$	3.18	4.09
$\text{NdSrFeO}_{4+\delta}$	3.27	4.14

Table 2

Linear TECs of the $\text{NdSrCo}_{1-x}\text{Fe}_x\text{O}_{4+\delta}$ samples calculated from the thermal expansion curves with temperature.

Composition	TEC ($\times 10^{-6}/^\circ\text{C}$)	
$\text{NdSrCo}_{0.6}\text{Fe}_{0.4}\text{O}_{4+\delta}$	16.9 ($40\text{--}500^\circ\text{C}$)	20.2 ($40\text{--}600^\circ\text{C}$)
$\text{NdSrCo}_{0.3}\text{Fe}_{0.7}\text{O}_{4+\delta}$	14.8 ($40\text{--}600^\circ\text{C}$)	
$\text{NdSrFeO}_{4+\delta}$	13.8 ($40\text{--}600^\circ\text{C}$)	

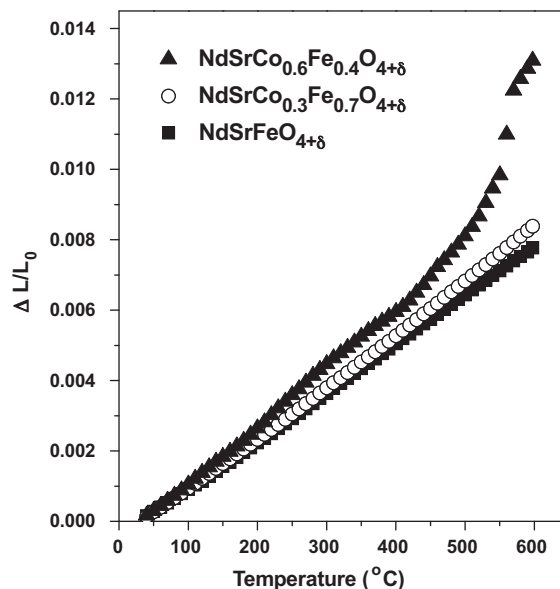


Fig. 2. Thermal expansion behaviors of the $\text{NdSrCo}_{1-x}\text{Fe}_x\text{O}_{4+\delta}$ samples sintered at 1300°C for 12 h.

exist in the intergrowth oxide structure. Since Fe ions are easy to form Fe^{4+} ion in B site of perovskite type oxides compared with Co ions [11], the mean valence of B site cations continuously increase with increasing Fe content as over $3+$

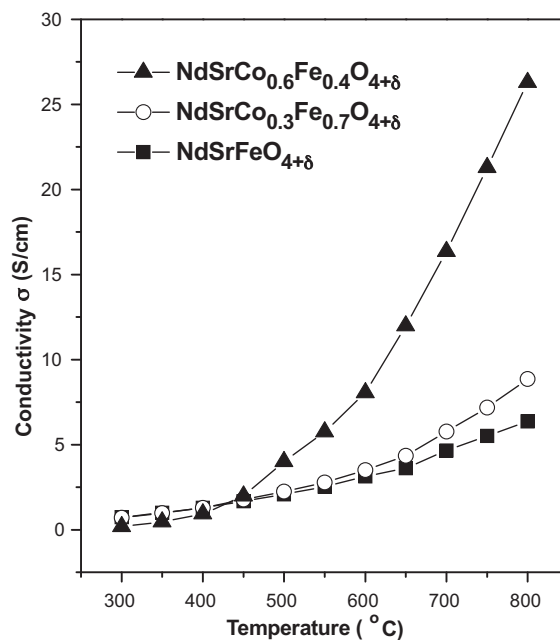


Fig. 3. Variations of the electrical conductivity of the $\text{NdSrCo}_{1-x}\text{Fe}_x\text{O}_{4+\delta}$ oxides measured in air atmosphere.

valence state, and it leads to increase the oxide ion content in the lattice to be electrically neutralized.

The thermal expansion behaviors of the intergrowth oxides sintered at 1300 °C for 12 h in the temperature range of 40–600 °C are shown in Fig. 2, and the calculated TEC values are listed in Table 2. It has been reported that the TEC of intergrowth oxide cathodes are generally lower than that of the perovskite oxides [7]. The values of TEC in this study are slightly higher than that in literatures. In case of the $x = 0.7$ and 1.0 samples, TEC values are much lower than the BSCF perovskite oxides, and comparable with the LSCF perovskite oxide [7]. Meanwhile, all samples indicate linear variation as function of temperature, except for the $x = 0.4$ composition with higher amount of Co ions. The $x = 0.4$ composition shows significant change at around 500 °C. The reason is assumed due to a spin transition from the smaller ionic radius of the low spin Co^{3+} ion ($r = 0.0545$ nm) to the high spin Co^{3+} ion ($r = 0.061$ nm) with increasing temperature [12,13], which

leads to an increase in TEC [14]. The substitution of Co by Fe induced to decrease TEC values.

The electrical conductivities of the intergrowth oxides measured in air atmosphere as a function of temperatures are illustrated in Fig. 3. The conductivities of all samples increased with increasing temperature, indicating thermally activated semiconductivity. With an increase in Fe content, the magnitude of the observed conductivity value decreased. It might be due to thermally activated Co ions. In the high temperature region, Co^{3+} ions in B site could transform into Co^{2+} and Co^{4+} ions [15]. The changed Co^{2+} and Co^{4+} ions create Co'_{Co} and $\text{Co}^{\bullet}_{\text{Co}}$ as charge carriers, respectively. This may effect to the conductivity values. The conductivity values of the intergrowth oxides are much lower than those of the perovskite type oxides with the same cations [16]. In the $x = 0.7$ and 1.0 samples, the conductivity are lower than 10 S cm^{-1} in entire temperature region between 300 and 800 °C, and the $x = 0.4$ sample with higher amount of Co ions shows relatively high

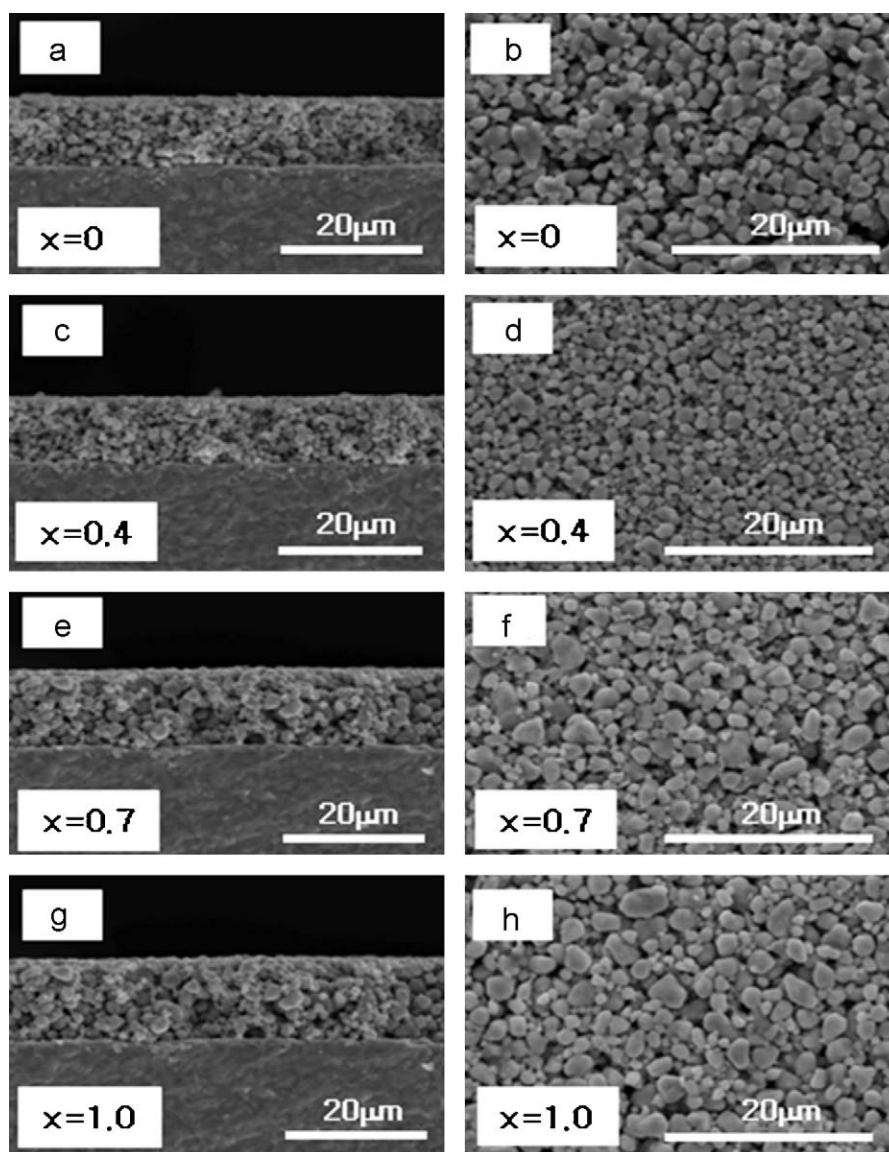


Fig. 4. SEM micrographs of the $\text{NdSrCo}_{1-x}\text{Fe}_x\text{O}_{4+\delta}$ cathodes on GDC electrolyte; (a), (c), (e), and (g): cross-sectional, and (b), (d), (f), and (h): surface images.

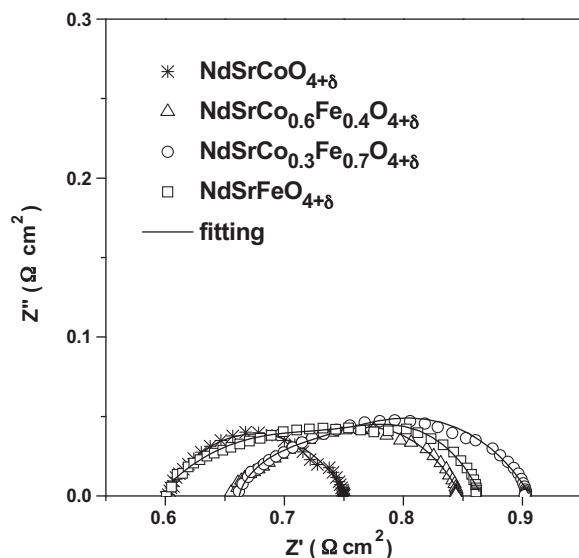


Fig. 5. Typical AC impedance spectra of the symmetrical half cells with GDC electrolyte in air atmosphere at 800 °C.

conductivity as over 25 S cm^{-1} at 800 °C, and the sample showed a remarkable increase in conductivity values after around 500 °C. This behavior is accordance with the significant increase in thermal expansion as shown in Fig. 2.

The top view and cross-sectional SEM micrographs of the $\text{NdSrCo}_{1-x}\text{Fe}_x\text{O}_{4+\delta}$ oxide cathodes on GDC electrolyte are shown in Fig. 4. Although the electrodes are sufficiently porous, and the thickness of the electrodes is proper to examine electrochemical performance as approximately 15 μm , the cathodes show only point contact among particles and poor adhesion between the cathode and the electrolyte. Therefore,

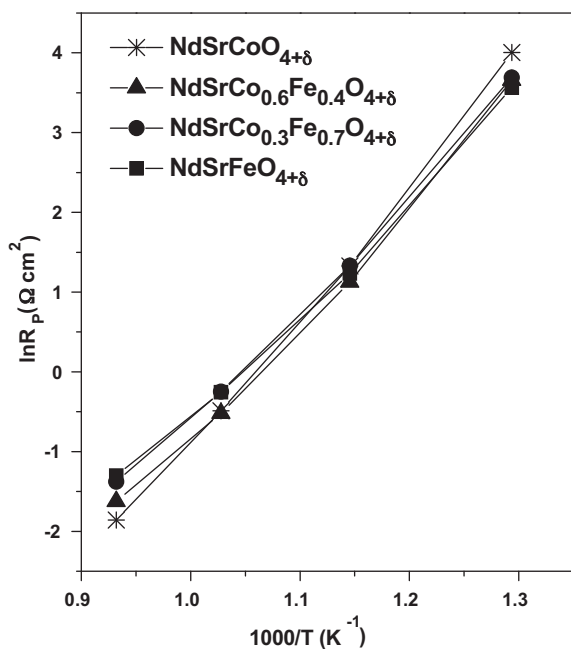


Fig. 6. Temperature dependence of polarization resistance (R_p) in air with the cathodes/GDC/cathodes symmetrical half cell, derived from the AC impedance data.

Table 3

Polarization resistance (R_p) at 800 °C and the calculated activation energy (E_a) of cathode samples in air atmosphere.

Composition	R_p at 800 °C ($\Omega \text{ cm}^2$)	E_a (eV)
$\text{NdSrCoO}_{4+\delta}$	0.16	1.40
$\text{NdSrCo}_{0.6}\text{Fe}_{0.4}\text{O}_{4+\delta}$	0.20	1.26
$\text{NdSrCo}_{0.3}\text{Fe}_{0.7}\text{O}_{4+\delta}$	0.25	1.21
$\text{NdSrFeO}_{4+\delta}$	0.27	1.16

higher firing temperature is required to prepare well sintered samples for polarization resistance measurement, and the optimization of firing conditions should be needed.

The electrochemical impedance data of the symmetrical half cells with GDC electrolyte and the cathodes in air atmosphere at 800 °C are shown in Fig. 5, and the temperature dependence of the polarization resistance (R_p , right intercept on Z_{re} axis – left intercept on Z_{re} axis) is shown in Fig. 6. Meanwhile, the calculated R_p and activation energy (E_a) in air atmosphere of all cathode samples are listed in Table 3. In the $\text{NdSrCo}_{1-x}\text{Fe}_x\text{O}_{4+\delta}$ oxide cathodes, the polarization resistance (R_p) values at 800 °C decreased with increasing Co content. As explained in Fig. 3, Co^{2+} and Co^{4+} ions are created in the high temperature region, if the generation of Co^{2+} ions is more dominant compared to Co^{4+} ions, oxide ion vacancies should be formed by Co'_{Co} to match electrical neutrality. The created oxide ion vacancies which is influenced to oxide ion permeability, and consequently oxygen reduction reaction [1,2], derive better electrochemical performance with increasing Co content. To be sure above assumption, X-ray photoelectron spectroscopy (XPS) and thermal analysis might be needed. However, the calculated activation energy increases with increasing Co content. It might be due to significant decrease in electrical conductivity in lower temperature region with increasing Co content as shown in Fig. 3.

Overall, the $\text{NdSrCo}_{1-x}\text{Fe}_x\text{O}_{4+\delta}$ oxides show possibility to be used as cathode materials for IT-SOFCs. However, low electrical conductivity and poor electrode microstructure of those materials need to be improved for good electrochemical performance.

4. Conclusions

$\text{NdSrCo}_{1-x}\text{Fe}_x\text{O}_{4+\delta}$ intergrowth oxide cathodes were prepared by glycine nitrate process, and all compositions show K_2NiF_4 type structure as a perovskite related intergrowth oxide. The introduction of Fe for Co leads to decrease TEC values and electrical conductivity, and increase polarization resistance and oxygen content. The electrical conductivities of all samples was $<30 \text{ S cm}^{-1}$ in the temperature range of 300–800 °C in air atmosphere. The $\text{NdSrCoO}_{4+\delta}$ composition showed the lowest polarization value of $0.16 \Omega \text{ cm}^2$ at 800 °C in air atmosphere, among the $\text{NdSrCo}_{1-x}\text{Fe}_x\text{O}_{4+\delta}$ ($0 \leq x \leq 1.0$) intergrowth oxide cathode materials. This indicates that the $\text{NdSrCoO}_{4+\delta}$ composition shows the best electrochemical performance compared with other compositions. The low conductivity and poor electrode microstructure of the cathode samples should be improved and need further investigation for better electrochemical performance.

Acknowledgements

This research was supported by Basic Science Research Program through the National Research Foundation of Korea (NRF) funded by the Ministry of Education, Science and Technology (grant number: 2010-0009130).

References

- [1] R.A. De Souza, J.A. Kilner, Oxygen transport in $\text{La}_{1-x}\text{Sr}_x\text{Mn}_{1-y}\text{Co}_y\text{O}_{3\pm\delta}$ perovskites. Part I. Oxygen tracer diffusion, *Solid State Ionics* 106 (1998) 175–187.
- [2] S.P. Jiang, Issues on development of $(\text{La},\text{Sr})\text{MnO}_3$ cathode for solid oxide fuel cells, *J. Power Sources* 124 (2003) 390–402.
- [3] K.T. Lee, A. Manthiram, $\text{La}_4\text{Sr}_3\text{Fe}_{3-y}\text{Co}_y\text{O}_{10-\delta}$ ($0 \leq x \leq 1.5$) intergrowth oxide cathodes for intermediate temperature solid oxide fuel cells, *Chem. Mater.* 18 (2006) 1621–1626.
- [4] K.T. Lee, D.M. Bierschenk, A. Manthiram, $\text{Sr}_{3-x}\text{La}_x\text{Fe}_{2-y}\text{Co}_y\text{O}_{7-\delta}$ ($0.3 \leq x \leq 0.6$ and $0 \leq y \leq 0.6$) intergrowth oxide cathodes for intermediate temperature solid oxide fuel cells, *J. Electrochem. Soc.* 153 (2006) A1255–A1260.
- [5] G. Amow, J. Au, I. Davidson, Synthesis and characterization of $\text{La}_4\text{Ni}_{3-x}\text{Co}_x\text{O}_{10\pm\delta}$ ($0.0 \leq x \leq 3.0$, $\Delta x = 0.2$) for solid oxide fuel cell cathodes, *Solid State Ionics* 177 (2006) 1837–1841.
- [6] A. Aguadero, J.A. Alonso, M.J. Escudero, L. Daza, Evaluation of the $\text{La}_2\text{Ni}_{1-x}\text{Cu}_x\text{O}_{4+\delta}$ system as SOFC cathode material with 8YSZ and LSGM as electrolytes, *Solid State Ionics* 179 (2008) 393–400.
- [7] M.A. Daroukh, V.V. Vashook, H. Ullmann, F. Tietx, I.A. Raj, Oxides of the AMO_3 and A_2MO_4 -type: structural stability, electrical conductivity and thermal expansion, *Solid State Ionics* 158 (2003) 141–150.
- [8] H.E. Shinawi, C. Greaves, Synthesis and characterization of the K_2NiF_4 phases $\text{La}_{1+x}\text{Sr}_{1-x}\text{Co}_{0.5}\text{Fe}_{0.5}\text{O}_{4-\delta}$ ($x = 0, 0.2$), *J. Solid State Chem.* 181 (2008) 2705–2712.
- [9] S.J. Skinner, J.A. Kilner, Oxygen diffusion and surface exchange in $\text{La}_{2-x}\text{Sr}_x\text{NiO}_{4+\delta}$, *Solid State Ionics* 135 (2000) 709–712.
- [10] C. Jin, J. Liu, Preparation of $\text{Ba}_{1.2}\text{Sr}_{0.8}\text{CoO}_{4+\delta}$ K_2NiF_4 -type structure oxide and cathodic behavior of $\text{Ba}_{1.2}\text{Sr}_{0.8}\text{CoO}_{4+\delta}$ -GDC composite cathode for intermediate temperature solid oxide fuel cells, *J. Alloys Compd.* 474 (2009) 573–577.
- [11] B. Liu, Y. Zhang, L. Tang, X-ray photoelectron spectroscopic studies of $\text{Ba}_{0.5}\text{Sr}_{0.5}\text{Co}_{0.8}\text{Fe}_{0.2}\text{O}_{3-\delta}$ cathode for solid oxide fuel cells, *Int. J. Hydrogen Energy* 34 (2009) 435–439.
- [12] P.M. Taccac, J.B. Goodenough, First-order localized-electron – collective-electron transition in LaCoO_3 , *Phys. Rev.* 155 (1967) 932–943.
- [13] V.G. Bhide, D.S. Rajoria, Y.S. Reddy, G. Rama Rao, G.V. Subba Rao, C.N. Rao, Localized-to-itinerant electron transitions in rare-earth cobaltates, *Phys. Rev. Lett.* 28 (1972) 1133–1136.
- [14] M. Mori, N.M. Sammes, Sintering and thermal expansion characterization of Al-doped and Co-doped lanthanum strontium chromites synthesized by the Pechini method, *Solid State Ionics* 146 (2002) 301–312.
- [15] V.V. Vashook, H. Ullmann, O.P. Olshevskaya, V.P. Kulik, V.E. Lukashevich, L.V. Kokhanovskij, Composition and electrical conductivity of some cobaltates of the type $\text{La}_{2-x}\text{Sr}_x\text{CoO}_{4.5-x/2\pm\delta}$, *Solid State Ionics* 138 (2003) 99–104.
- [16] K.T. Lee, A. Manthiram, Characterization of $\text{Nd}_{0.6}\text{Sr}_{0.4}\text{Co}_{1-y}\text{Fe}_y\text{O}_{3-\delta}$ ($0 \leq y \leq 0.5$) cathode materials for intermediate temperature solid oxide fuel cells, *Solid State Ionics* 176 (2005) 1521–1527.